APPLICATION OF SELF-MIXING INTERFEROMETRY FOR DEPTH MONITORING IN THE ABLATION OF TiN COATINGS

Paper M905

Ali Gökhan Demir[1], Barbara Previtali[1], Alessandro Magnani[2], Alessandro Pesatori[2], Michele Norgia[2]

[1]Department of Mechanical Engineering, Politecnico di Milano, Via La Masa 1, 20156 Milan, Italy
[2]Department of Electronics and Information, Politecnico di Milano, Via Ponzio 34/5, 20133 Milan, Italy

Abstract

Among possible monitoring techniques, self-mixing interferometry stands out as an appealing option for online ablation depth measurements. The method uses a simple laser diode and interference is detected inside the diode cavity and measured as the optical power fluctuation by the photodiode encased in the laser diode itself. This way, self-mixing interferometry combines the advantages of a high resolution point displacement measurement technique, with high compactness and easiness of operation. For a proper adaptation of self-mixing interferometry use in laser micromachining to monitor ablation depth, certain optical, electronical and mechanical limitations need to be overcome. In laser surface texturing of thin ceramic coatings the ablation depth control is critically important to avoid damage by substrate contamination. In this work, self-mixing interferometry was applied in the laser percussion drilling of TiN coatings. The ~4 µm thick TiN coatings were drilled with a 1 ns green fibre laser, while the self-mixing monitoring was applied with a 785 nm laser diode. The limitations regarding the presence of process plasma are discussed. The design criteria for the monitoring device are explained. Finally, the self-mixing measurements were compared to a conventional optical measurement device. The concept was validated as the measurements were statistically the same.

Introduction

Laser texturing or patterning of surfaces generates functional properties, which can be exploited to improve adhesion [1], optical [2], wetting [3] and tribological [4] properties. Applied in the form of shallow dimples, laser surface texturing can improve wear and friction properties of the surface significantly [4]. One of the most important design parameters of the surface texture is the depth of the dimple. The control over the dimple depth in laser ablation is a critical point especially, when texturing is applied to thin, ceramic surface coatings. The coating thickness varies in the range of a few µm and the laser machining should not cause damage by machining through the coating and reaching the substrate [5]. The delicacy of the machining conditions can be overcome by careful study of the main laser processing parameters such as pulse energy, repetition rate and number. On the other hand online monitoring capabilities are required to overcome process variations during the machining of large area components.

In literature several monitoring strategies for ablation depth measurement have been proposed, using the acoustic emission of the process [6] and mechanical vibration due to wavefront expansion [7], whereas optical measurement methods have received more attention due to fast and high precision measurement they provide. The different optical methods used for depth measurement can provide either direct or indirect measurement of the ablation depth. Use of photodiodes [8,9] and optical emission spectrum [10-14] are the indirect methods that enable to correlate the signal to the measured depth or change of material layer by observing the presence of a new signal component. Direct measurements can be achieved via high resolution imaging systems that allow visualization of ablation depth in transparent materials [15]. On the other hand, interferometric methods can be implemented to measure the ablation depth, at the end of the process, as well as during the process itself. White light interferometry implemented into the optical chain of the processing laser gives the possibility to acquire high resolution 3D images of the ablation area [16]. Being an offline measurement strategy this method does not give the possibility to compensate the processing deviations. More recently faster techniques based on Fourier domain optical coherence tomography (OCT) [17-19] and self-mixing interferometry [20-22] have been proposed as solutions for ablation depth monitoring. Both of the techniques allow high speed measurement by providing data over only a single dimension, which is depth. In Fourier domain OCT interference pattern is measured with a spectrometer to divide the pattern in its spectral components. The

Fourier transform of the spectrum yields the position information of all the illuminated area, without a distinction in lateral position. Depth and time resolution of the measurement method has been demonstrated to be 6.2 µm and 100 ns respectively. Differently, self-mixing interferometry is a method based on optical feedback. The self-mixing phenomenon occurring in the laser cavity is exploited to measure displacement. The reflected light from a target surface interferes with the laser light in the cavity, which is measured as the optical power fluctuations. The method allows sub-micrometre measurement as the resolution is intrinsically half of the measurement laser wavelength (λ/2). The technique has been employed in laser microdrilling using a ps pulsed source as the processing beam. However, coherent detection of this kind is prone disturbances, which are expected to occur passing through turbid media [23]. In laser micro machining, the ablation plasma constitutes the turbid media and is characterized by high pressure, temperature, and refraction index variations. These problems have not been yet addressed in the literature.

In this work, an ablation depth monitoring system based on self-mixing interferometry is developed. The system is aimed to measure the microdrilling depth on a ceramic TiN coating with 4 µm thickness. The system design is explained first and then optical, electronical and mechanical limitations regarding the measurement feasibility are tackled. After the determination of the measurement feasibility, the measurement performance was validated by confronting the measurement results with an industrial surface measurement system.

Self-mixing interferometry system

Self-mixing interferometry uses principal of interference occurring in the laser cavity (see Figure 1). Conventionally, laser diodes (LD) equipped with a photodiode (PD) for output power monitoring are employed to construct self-mixing interferometers. Therefore compared to the conventional Michelson interferometer, which uses a reference and a measurement arm, the system is less complicated.

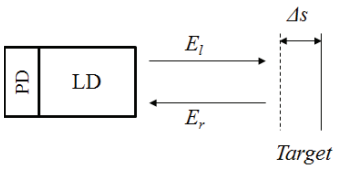

Figure 1. Conventional laser diode self-mixing configuration

As depicted in Figure 1, in a self-mixing interferometry configuration the power back reflected from a remote target enters the cavity after being attenuated in the external cavity. The reflected laser field possesses phase component that depends on the distance of the reflecting body at a given time instance, expressed as [24]:

$$\varphi_r(t)=2\cdot k\cdot s(t) \quad (1)$$

with

$$k=2\pi/\lambda \quad (2)$$

and s(t) is the distance of the remote target at a given time instance. The back reflected field E_r, adds to the lasing field E_0. Therefore the lasing field amplitude and frequency are modulated by the phase φ_r. This interferometric phase (φ_i) can be retrieved from the change of the optical power measured by the photodiode attached to the back of the laser diode, and a measurement of the target displacement can be made. Essentially at each displacement of half laser wavelength (λ/2) a fringe forms resulting in a saw-tooth like signal overall. By fringe counting the total displacement is calculated.

On the other hand, the periodic function of the interferometric phase depends on the feedback parameter C. Essentially the feedback parameter determines the signal shape and is correlated to the optical attenuation in the external cavity. For interferometric displacement measurement that are non ambiguous in direction, the feedback parameter is required to be operated at the moderate regime ($1<C<4.6$). Accordingly, the measurement system is highly sensitive to the amount of back reflected light as lower intensity of back reflected light will cause direction ambiguity, whereas high amount of back reflected light will cause mode-hopping in the laser diode, thus cancelling the measurement capability. In usual practice, the feedback parameter is controlled empirically by adjusting an attenuator to limit the amount of back reflected light entering the cavity. In laser micromachining, the amount of reflected light is highly variable in time due to all the perturbations occurring in the ablation zone. The surface characteristics change and ablation plasma can scatter the incoming interferometer.

The particular system employed in this study consisted of two laser sources: 1- the processing and 2- the measurement laser. The processing beam was a fibre laser with MOPA architecture operating with 532 nm wavelength and 1.2 ns pulse duration (YLPG-5 from IPG Photonics). The laser operated between 20-300 kHz repetition rates with maximum

pulse energy of 20 µJ, estimated maximum peak power of 16 kW and maximum average power of 6 W. The two beams were combined and launched onto the workpiece on the same point (see Figure 2). With 3.49 mm collimated beam diameter, M^2=1.1, and 100 mm focal lens, the focused beam diameter was calculated as 21.7 µm. The ablation front displacement was measured by the self-mixing interferometer. The total number of fringes showed the ablation depth. For the present application the system was supposed to have sub-micrometre depth resolution to resolve the drilling depth on 4 µm thick TiN coating. Moreover, the time resolution was required be adequate to capture the fast ablation phenomenon. Accordingly the system design had to fulfil a series of optical, electrical and mechanical requirements.

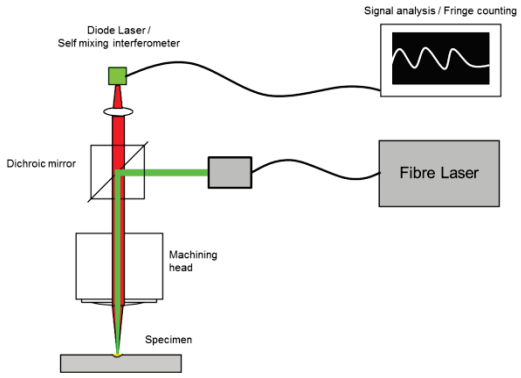

Figure 2. The scheme of laser self-mixing interferometry system for ablation depth monitoring.

Requirements of the monitoring method and regarding limitations

Optical requirements: The selection of the wavelength of the interferometer determines the intrinsic resolution of the device as fringes will be completed at each λ/2 displacement. On the other hand, small wavelengths would require faster electronics, thus larger bandwidth to be able to acquire more fringes for the same process duration. It should be noted that signal processing can be applied to improve the time resolution of the measurement to more than λ/2.

The wavelength of the interferometer beam also determines the beam waist diameter. Smaller wavelengths can produce smaller spot diameters, which can potentially improve the spatial resolution of the device. The two beams (processing and measurement) should be matched to obtain same focal position for both the beams, or have overlapping depth of focus regions. This, in fact is a challenging issue as the beams are focused through the same focal lens, which would produce different focal positions for the two different wavelengths due to chromatic aberration. The self-mixing interferometry laser should also possess sufficient depth of focus or namely Rayleigh range.

Figure 3 shows an example of emission spectrum during TiN ablation. It can be observed that the ablation emission is concentrated in visible and UV range, while in the IR region the contribution is not present. Furthermore, Ti I and Ti II emission lines are clearly evident. In order to avoid interference with the plasma emission the wavelength band between 300-750 nm requires to be avoided.

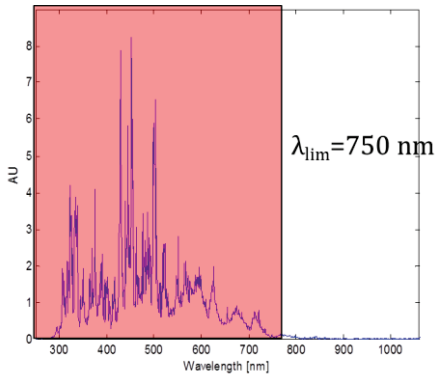

Figure 3. An example to the emission spectrum in laser ablation of TiN coating.

Electrical requirements: The device should be able to capture the fast ablation phenomenon, occurring in ns-µs scale. This requires fast electronics with high signal to noise ratio, so that fringes can be visible without any aliasing effects. The main parameter determining the speed of signal acquisition is the bandwidth of the electronics used in the self-mixing interferometer. Another contrasting issue with bandwidth is that it is reduced with high signal amplification. Therefore, bandwidth (BW) has to be considered as a fundamental design parameter for self-mixing interferometry in ablation depth monitoring. A simple relationship can be derived using the wavelength of the self-mixing interferometer (λ_{int}) and average material removal rate (MRR) to calculate the time to observe a single fringe (t_{frg}) from:

$$t_{frg}=\lambda_{int}/(2\cdot MRR) \qquad (3)$$

In order to avoid aliasing of the signal the Nyquist criteria has to be fulfilled. Therefore the minimum acquisition frequency (f_{min}) is:

$f_{min}=2/t_{frg}$ (4)

As a matter of fact for adequate signal representation, the bandwidth of the self- mixing interferometer is required to be sufficiently larger than the minimum acquisition frequency, f_{min}. Estimation of f_{min} based on previously observed MRR (2 µm/25 pulses) and using the shortest wavelength usable to avoid interfering with the plasma emission (750 nm) shows that BW>23 kHz.

Mechanical requirements: The mechanical requirements involve the stability of the components used in the setup, the possibility of flexible alignment, and protection from mechanical vibrations from the environment. Due to high sensitivity of the measurement method external vibrations can be also acquired during the measurement.

Implemented system characteristics

The self-mixing interferometry was integrated in house using off-the-shelf components. In particular, the light source used was a GaAlAs laser diode with a multi-quantum well structure (Hitachi HL7851G). The built-in monitor photodiode allowed the measurement of the self-mixing interference. The exiting beam was in elliptical shape that is characteristic for single transverse electronic mode laser diode beams. Single mode laser diodes are considered to have M^2 values between 1.1-1.2 [25]. The output power in CW emission was 15 mW. The laser diode was used with a 10 mm collimation lens and was integrated into a single stage trans-impedance operational amplifier. The bandwidth of the interferometer was 35 MHz, which is sufficiently enough to acquire the fast ablation phenomenon.

To combine the collimated beam in free space a longpass dichroic mirror with 50% transmission/reflection point at 567 nm was chosen (Thorlabs DMLP567). A bandpass filter at 780 nm central wavelength and ±10 nm FWHM bandwidth was employed after the collimation stage of the interferometer (Thorlabs FBH780-10). This allowed filtering out any other optical component to be measured by the photodiode of the laser diode. A diaphragm was implemented to control the amount of returning light into the laser cavity, which is essential to control the feedback parameter (C). In order to compensate for chromatic aberration an achromatic doublet lens with 100 mm focal distance was chosen that provided a 317 µm focal position difference between the wavelengths of processing and measurement lasers. Within the given configuration, the self-mixing interferometry beam diameter was calculated as 41.4 µm in fast axis and 23.5 µm in slow axis. Although the beam is larger in fast axis compared to the processing beam, the highest intensity portion of the measurement beam passes to the bottom of the hole. This high intensity part of the beam advances to the bottom of the hole, whereas the lower intensity portion remains on the material surface. Surface perturbations may cause changes in the signal; however, the higher intensity part dominates the way the fringe patterns are observed.

Table 1 Electrical and optical characteristics of the self-mixing interferometry system

Electrical	
Output power	15 mW
Bandwidth	35 MHz
RMS voltage output noise	5 mV
Optical	
Depth resolution (λ/2)	0.3925 µm
Focused fast axis beam diameter	41.4 µm
Focused slow axis beam diameter	23.5 µm
Rayleigh range in fast axis	1426 µm
Rayleigh range in slow axis	461 µm

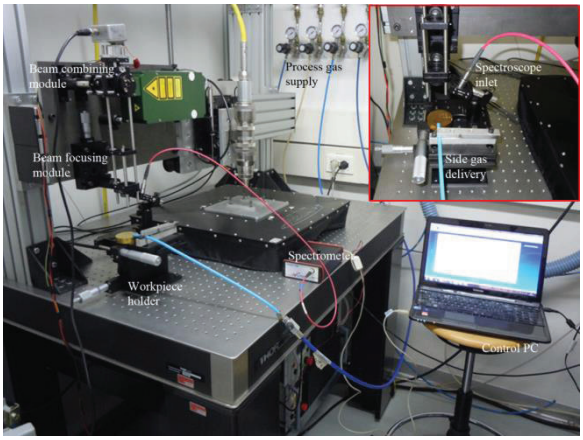

Figure 4. Experimental setup for laser self-mixing interferometry for ablation depth monitoring on TiN coating.

The self-mixing interferometry signal was captured with a digital oscilloscope digital with 350 MHz maximum bandwidth, 5 GS/s sampling rate and $16{\cdot}10^6$ record length (Tektronix TDS5034B). Table 1 summarizes the general characteristics of the interferometry system, whereas Figure 4 illustrates the implemented system.

Monitoring of dimple depth in microdrilling of TiN coated 39NiCrMo3 steel

Monitoring system was tested on TiN coating applied on 10 mm thick 39NiCrMo3 steel. This combination represents the coated tool steels, for which LST is applied to reduce friction and wear. Laser percussion drilling was applied with the green pulsed fibre laser. The laser source provided the advantages of using shorter pulse duration and shorter wavelength, leading in reduced thermal interaction in ns regime. Pulsed green laser sources have been studied previously in the literature showing improved machining quality and removal rates compared to near IR sources [26-28]. The machined TiN coating absorptivity weakly depends on the wavelength between visible and near IR regions [29], however the shorter wavelength intrinsically provides smaller focused beam. Thus, high intensity is achievable despite the low pulse energy (F=10.4 J/cm^2; I=8.7 GW/cm^2). In order to achieve high quality dimples, the use of low energy pulses is advantageous. However, in order to achieve significant dimple depth a train of pulses is required. Accordingly each dimple is realized by percussion drilling. Percussion drilling with multiple pulses is the basis of the point-by-point laser surface texturing (LST) strategy. In this strategy a train of pulses is sent on a stationary point to realize a shallow dimple and moved to the next position. The dimple spacing is maintained with higher precision with such strategy, with the expense of reduced productivity compared to on the fly machining [30]. During the monitoring study single dimples were realized at a time. The study consisted of two phases 1- effect of the side gas and determination of stable measurement signal conditions and 2- evaluation of the measurement performance.

Determination of stable measurement signal conditions

The initial experiments carried out in ambient air revealed signals with moderate amplitude, with well-defined saw tooth shape fringes in both ascending and descending directions (see Figure 5a). The number of fringes in both directions appeared to be equal, resulting in null displacement. Moreover, the fringes within the laser emission duration showed ascending movement, whereas the ablation front should advance in the opposite direction. This phenomenon was repeatedly observed with different microdrilling conditions. It was concluded that the observed phenomenon did not belong to the ablation front displacement. It is plausible that the fringe appearance can be caused by another phenomenon causing refractive index change such as the ablation plasma, plume and shock wave. As a matter of fact, the signals showed fringe movements start corresponding to the end of the laser emission delay. The emission delay is a characteristic of the laser source, which is caused by the optical and electronical delays generated at the pumping stage of the active media. The emission delay has been characterized previously for different parameter combinations, which are not reported here for brevity. The example shown in Figure 5a clearly shows the signal displacement start around the end of the laser emission delay (t_d=514±13 µs), which corresponds to the ablation initiation. It can be observed that the displacement in the opposite direction occurs after the end of the laser emission, as indicated by the end of the laser gate. As a matter of fact the plasma generated shock wave expansion can occur in durations much longer than the ablation itself [31], which can cause the present fringe appearance.

In ambient atmosphere, it is plausible that the self-mixing laser beam interacts with the ablation plasma and shock wave. All these components around the ablation region cause change in refraction index locally. As a consequence the optical distance changes and the phenomenon is observed as the ascending movement of the fringes. At the end of the laser emission the ablation region clears out to return to ambient conditions. Thus the refraction index returns to the one belonging to the air, which is observed as the descending movement. To overcome the plausible effects of the ablation plume, side gas parallel to the material surface and perpendicular to the measurement and processing beams was used. Because the ambient air is composed majorly of N_2 molecules, this gas was chosen to not alter the refraction index significantly, and it was preferred over compressed air due to its inert properties. The outcome was the observation of a signal with low amplitude fringes occurring in the descending direction. The start of fringe occurrence coincided with the end of the emission delay of the processing delay. Figure 5b shows an example signal acquired while N_2 side gas at 1 bar was in use. In particular the signal shows 8 fringes in descending direction, showing a displacement of 3.14 µm. The used processing conditions yielded a dimple depth of 3.43 ± 0.5 µm.

The fact that the self-mixing interferometry measurement was in the expected dimple depth range gave way to the further hypothesis on the interaction between the material, processing and measurement beams. It can be expected that the side gas may

provide two effects that allow the passage of the measurement beam to observe the dimple bottom, thus the ablation front displacement.

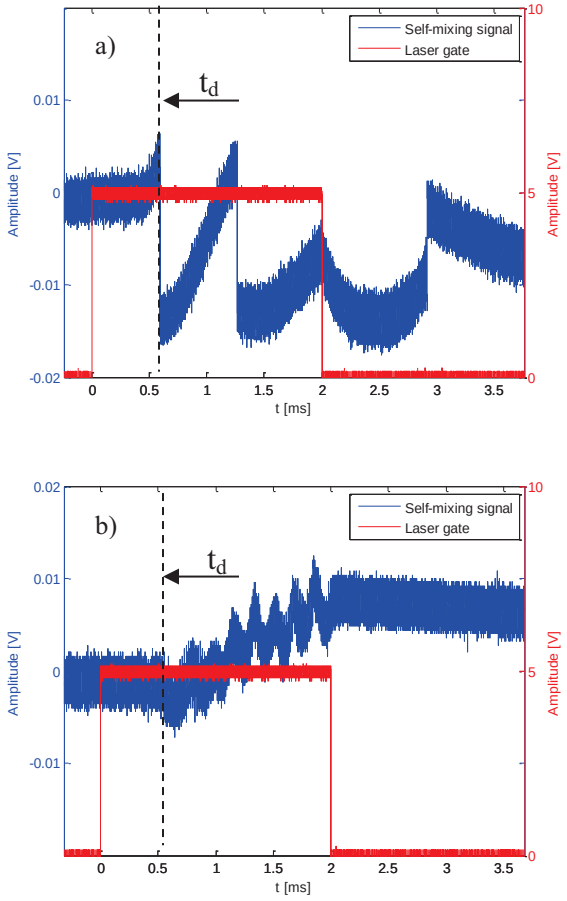

Figure 5. The effect of side gas on the self-mixing interferometry signal characteristics. Processing laser parameters are E=19.3 µJ, PRR=50 kHz, N=75. a) Processing in ambient atmosphere, b) processing with N_2 side gas with 1 bar pressure.

- Extinguishing effect: The side gas can maintain a higher ionization threshold, allowing generation of less amount of plasma and the resulting ablation plume could be expected to be less dense, causing minor changes in the refraction index, therefore the measurement beam reaches the dimple bottom without significant coherence loss.

- Deviation effect: The side gas may provide mechanical effect of moving the generated ablation plasma away from the dimple opening, allowing the major part of the measurement beam to avoid passing through it. Thus, the change in optical path due to the refraction index change is partially avoided, and the greater part of the measurement beam reaches the bottom of the dimple.

The extinguishing effect would in fact require ambient conditions either free of gas, or inert gases with ionization potentials much higher than the one belonging to air. The ionization potentials of air and N_2 are very similar, being 14.9 eV and 15.6 eV respectively, whereas for instance He has an ionization potential of 24.6 eV [32]. Callies et al. have calculated surface pressure during the ablation of Cu target with 60 ns pulses [33]. The authors reported that surface pressure returns to ambient conditions soon after the end of the pulse duration, at around 100 ns. Therefore the used gas pressure can suffice for divert the ablation plume. Accordingly the deviation effect seems to be the more plausible. Further investigations are carried out on this matter.

Evaluation of the measurement performance with an offline measurement device

The measurement performance of self-mixing interferometry was compared to an industrial surface topography and geometry measurement device, Alicona InfiniteFocus that is based on the focus variation microscopy (FVM). The device is capable of providing depth resolution down to 0.01 µm, and lateral resolution down to 0.44 µm. After the acquisition the dimple depth was determined as the deepest point of the dimple with respect to the surface. An example of dimple depth measurement procedure is explained in Figure 6.

The self-mixing interferometry measurements required the use of side gas. As a matter of fact the addition of gas has to be treated as an additional factor. Therefore, within the comparative study 3 treatment groups had to be considered. The comparison groups in the end were 1- focus variation microscopy on dimples microdrilled without the side gas, 2- focus variation microscopy on dimples microdrilled with the side gas, and 3- self-mixing interferometry on dimples drilled with the side gas. N_2 was used at 1 bar pressure as the side gas. An experimental design was conducted to test the statistical significance of difference of the measurement depth between the different treatment groups.

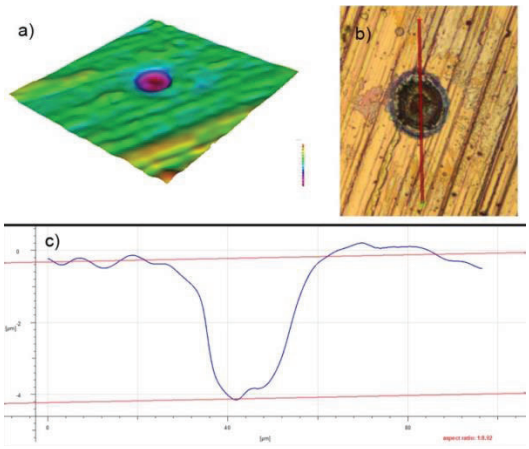

Figure 6. The dimple depth measurement procedure with focus variation microscopy system. a) The acquired dimple in 3D representation, b) the section of measurement passing through dimple centre, c) the section profile along with the fitted planes for the top and bottom of the dimple.

Table 2 Experimental design for the comparison of measurement performance of self-mixing interferometry against focus variation microscopy.

Fixed parameters	**Symbol**	**Levels**
Pulse energy	E [µJ]	19.3
Focal height	h_f [mm]	0
Pulse repetition rate	PRR[kHz]	50
Varied parameters	**Symbol**	**Levels**
Number of effective pulses	N	25, 75, 100, 125
Measurement condition (block)	Type	FVM - without gas FVM – N_2, 1 bar SMI – N_2, 1 bar
Measured variable	**Symbol**	
Dimple depth	h [µm]	

The dimples were drilled with a single combination of processing laser energy (E) and pulse repetition rate (PRR), whereas the number of pulses (N) was varied to study increasing depth. Because the comparison groups were realized in different time occasions, they were treated as blocks, with the hypothesis that there is no interaction with the other parameter in the experimental plan. Five replications were made for the conditions using focus variation microscopy. For the self-mixing interferometry condition at least 7 replications were made due to higher variability observed in the acquired signals.

Focus variation microscopy acquisitions were made with 50X magnification, and 0.02 µm lateral resolution. Whereas for self-mixing interferometry the depth measurement was based on manual fringe counting after a low-pass digital filtering stage (cut-off frequency 50 kHz, with 3rd order Butterworth window). Table 2 summarizes the fixed and varied parameters, along with the measured variable belonging to the employed experimental plan.

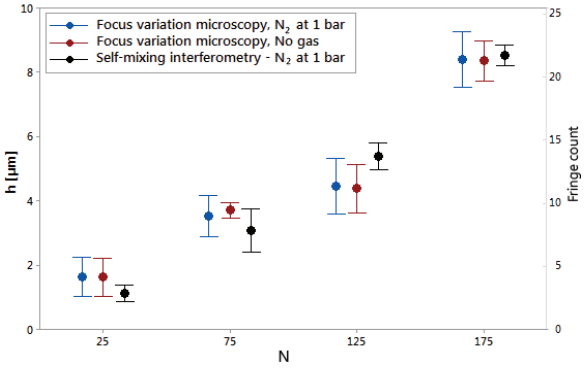

Figure 7. Dimple depth as a function of number of pulses and measurement conditions. The ordinate on the right hand side represents the dimple depth in equivalent fringe count. Error bars represent 95% confidence interval for the mean.

Figure 7 depicts all the measured dimple depths belonging to different conditions. The dispersion of all the data points suggests that all measurement conditions report the same range of depth. This observation was confirmed by the Analysis of Variance. The significance of effect of the measurement condition is rejected by a very high p-value (0.978), confirming that there is no statistical difference between self-mixing interferometry and focus variation based microscopy measurements. Additionally, this confirms that there is no significant effect of the side gas on the drilled hole depth. Additionally, the study shows increased material removal rate after the reach of substrate below 4 µm drilling depth (N=125). The capability of ablation depth measurement with self-mixing interferometry is demonstrated in case of changing material layers, which are characterized by different optical properties.

Discussion

The statistical study confirms the validity of the self-mixing interferometry measurements. However, it

should be noted that the comparison were made on a large quantity of replicates, with a relatively variable process. As a matter of fact, the standard error of the process calculated in the Analysis of Variance was larger than the resolution of the self-mixing interferometer just by a small amount (S=0.585 μm). Moreover, due to restriction, the comparison was based on populations, rather than the same dimples measured by two different devices. More investigation regarding the measurement error on a single drilled hole is underway. For large area surface texturing purposes, measurements based on a number of replications can be accepted. For applications regarding deeper holes (aspect ratio>1-5), the variance of measurement is also at acceptable level. On the other hand exact measurement on singular shallow holes is not viable due to low intrinsic resolution of the method.

Although it has not been the primary concern of the work, it is duly noted that an immediate integration of the monitoring system in an industrial environment does not seem possible. For robust functioning of the system, alignment sensitivity of the two beams has to be confronted. Other limitations regarding the use of this method rely on the data analysis. The method requires high resolution acquisitions in very short scale of time. For real-time implementation, also data processing speed should be matched. In order to use integrated electronics, the signal quality is required to be increased as well.

Conclusions

This work reported the development of a self-mixing interferometry system to monitor ablation depth on thin ceramic surface coatings. The online measurement system was implemented by combining the self-mixing interferometry beam with the processing beam and launching them together to the processing zone. The implemented system was characterized by 0.4 μm depth and 29 ns time resolution. The system for measuring the displacement of the ablation front was validated in fast ablation conditions with limited machining depth. The critical point in the measurement remains with the fact that the used coherence detection method is prone to disturbances caused by the turbid media around the ablation zone. The problem has been resolved by the use of a side gas jet, which is expected to divert the ablation plume and allow the measurement beam to pass into the drilled microhole. Another possible explanation to the effect of the side gas is the extinguishing effect, however it is found to be less likely due to the similarity of the used gas type (N_2) compared to air in terms of plasma threshold.

If the sensitivity issues can be resolved, the implemented method shows promise as a simple and cost effective method for depth monitoring in laser micromachining applications. Self-calibrating processes or close loop control of laser micromachining by integrating the interferometry signal to the automation system are possibilities that the method can provide.

References

[1] Man, H.C., Chiu, K.Y., Guo, X. (2010) Laser surface micro-drilling and texturing of metals for improvement of adhesion joint strength, Applied Surface Science 256, 3166–3169

[2] Abbott M., Cotter, J. (2006) Optical and electrical properties of laser texturing for high-efficiency solar cells, Prog. Photovoltaics Res. Appl., 14 (3), 225–235

[3] Kietzig, A.-M., Hatzikiriakos, S. G., Englezos, P. (2009) Patterned superhydrophobic metallic surfaces, Langmuir, 25 (8), 4821–7

[4] Etsion, I. (2005) State of the Art in Laser Surface Texturing, J. Tribol., 127 1, 248

[5] Demir, A.G., Lecis, N., Previtali, B., Ugues D. (2013) Scratch resistance of fibre laser surface textured TiN coatings, Surface Engineering, 29 (9), 654-659

[6] Kurita, T., Ono, T., Nakai, T. (2001) A study of processed area monitoring using the strength of YAG laser processing sound, Journal of Materials Processing Technology 112, 37-42

[7] Stafe, M., Negutu, C., Popescu, I.M. (2005) "Real-time determination and control of the laser-drilled holes depth," Shock Waves, 14 (1-2), 123-126

[8] Hand, D.P., Peters, C., Haran, F.M., Jones, J.D.C. (1997) A fibre-optic-based sensor for optimization and evaluation of the laser percussion drilling process, Measurement Science and Technology, 8, 587-592

[9] Stournaras, A., Salonitis, K., Chryssolouris, G., (2010) Optical emissions for monitoring of the percussion laser drilling process, International Journal of Advanced Manufacturing Technology, 46 (5-8), 589-603

[10] Kanicky, V., Musil, J., Mermet, J.-M. (1997) Determination of Zr and Ti in 3- mu m-Thick ZrTiN Ceramic Coating Using Laser Ablation Inductively Coupled Plasma Atomic Emission Spectrometry, Applied Spectroscopy, 51 (7), 1037-1041

[11] Papazoglou, D.G., Papadakis, V., Anglos, D., (2004) In situ interferometric depth and topography monitoring in LIBS elemental profiling of multi-layer structures, Journal of Analytical Atomic Spectrometry, 19, 483–488

[12] Balzer, H., Hoehne, M., Sturm, V., Noll, R., (2005) Online coating thickness measurement and depth profiling of zinc coated sheet steel by laser-induced breakdown spectroscopy, Spectrochimica Acta Part B, 60, 1172–1178

[13] Grisolia, C., Semerok, A., Weulersse, J., Leguern, F., Fomichev, S., Brygo, F., Fichet, P., Thro, P., Coad, P., Bekris, N. (2007) In-situ tokamak laser applications for detritiation and co-deposited layers studied, Journal of Nuclear Materials 363–365, 1138–1147

[14] Ruiz, J., González, A., Cabalín, L.M., Laserna, J.J., (2010) On-line laser-induced breakdown spectroscopy determination of magnesium coating thickness on electrolytically galvanized steel in motion, Applied Spectroscopy, 64 (12), 1342-1349

[15] Döring, S., Richter, S., Nolte, S., Tünnermann, S. (2011) in Proc. of SPIE Vol. 7925 Frontiers in Ultrafast Optics: Biomedical, Scientific, and Industrial Applications XI, San Francisco, California, USA, 792517 (8 pp)

[16] Stournaras, A., Salonitis, K., Chryssolouris, G., (2010) Optical emissions for monitoring of the percussion laser drilling process, International Journal of Advanced Manufacturing Technology, 46 (5-8), 589-603

[17] Webster, P.J.L., Yu, J.X.Z., Leung, B.Y.C., Anderson, M.D., Yang, V.X.D., James, M., (2010) In situ 24 kHz coherent imaging of morphology change in laser percussion drilling, Optics Express, 35 (5), 646-648

[18] Webster, P.J.L., Wright, L.G., Mortimer, K.D., Leung, B.Y., Yu, J.X.Z., Fraser, J.M. "Automatic real-time guidance of laser machining with inline coherent imaging," Journal of Laser Applications, 23 (2), 022001-1-022001-6

[19] Leung, B.Y.C., Webster, P.J.L., Fraser, J.M., Yang, V.X.D., (2012) "Real-Time Guidance of Thermal and Ultrashort Pulsed Laser Ablation in Hard Tissue Using Inline Coherent Imaging," Lasers in Surgery and Medicine 44, 249–256

[20] Mezzapesa, F.P., Ancona, A., Sibillano, T., De Lucia, F., Dabbicco, M., Maurizio, L., Pietro, M., Scamarcio, G. (2011) High-resolution monitoring of the hole depth during ultrafast laser ablation drilling by diode laser self-mixing interferometry, Optics Letters, 36 (6), 822-824

[21] Spagnolo, V., Ancona, A., Scamarcio, G., (2012) Detection of ultrafast laser ablation using quantum cascade laser-based sensing, Applied Physics Letters, 101, 171107-1-171107-4

[22] Mezzapesa, F.P., Sibillano, T., Di Niso, F., Ancona, A., Lugarà, P., Dabicco, M., Scamarcio, G., (2012) Real time ablation rate measurement during high aspect-ratio hole drilling with a 120-ps fiber laser, Optics Express, 20 (1), 663-671

[23] Dunsby, C., French, P.M.W. (2003) Techniques for depth-resolved imaging through turbid media including coherence-gated imaging, J. Phys. D. Appl. Phys., 36 (14), R207–R227

[24] Giuliani, G., Norgia, M., Donati, S., Bosch, T., (2002) Laser diode self-mixing technique for sensing applications, J. Opt. A Pure Appl. Opt., 4 (6), S283–S294

[25] Sun, H. (2012) Laser Diode Beam Basics, Manipulations and Characterizations, Springer, New York

[26] Chang J.J., Warner B.E., Dragon E.P., Martinez M.W. (1998) Precision micromachining with pulsed green lasers, Journal of Laser Application 10 (6), 285-291

[27] Tunna L., Kearns, A., O'Neill, W., Sutcli, C.J., (2001) Micromachining of copper using Nd :YAG laser radiation at 1064, 532, and 355 nm wavelengths, Optics & Laser Technology 33, 135–143

[28] Knowles M.R.H., Rutterford G., Karnakis D., Ferguson A. (2007) Micro-machining of metals, ceramics and polymers using nanosecond lasers, Int J Adv Manuf Technol 33, 95–102

[29] Kononenko T.V., Garnov S.V., Pimenov S.M., Konov V.I., Romano V., Borsos B., Weber H.P. (2000) Laser ablation and micropatterning of thin TiN coatings, Appl. Phys. A 71, 627–631

[30] Demir A.G., Previtali B., Lecis N. (2013) Development of laser dimpling strategies on TiN coatings fortribological applications with a highly energetic Q-switched fibre laser, Optics & Laser Technology 54, 53–61

[31] Zhou, Y., Benxin, W., Tao, S., Forsman A., Gao, Y. (2011) Physical mechanism of silicon ablation with long nanosecond laser pulses at 1064nm through time-resolved observation, Appl. Surf. Sci., 257, 2886-2890

[32] Sun, J., Longtin, J.P. (2001) Inert gas beam delivery for ultrafast laser micromachining at ambient pressure, J. Appl. Phys., 89 (12), p. 8219

[33] Callies, G., Berger, P., Huegel, H (1995) Time-resolved observation of gas-dynamic discontinuities arising during excimer laser ablation and their interpretation, J. Phys. D: Appl. Phys., 28, 794-806